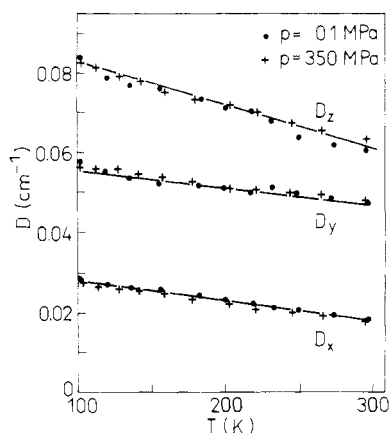


**Figure 1.** Temperature variations of the powder spectra recorded at 9.42 GHz under atmospheric pressure ( $p = 0.1$  MPa). Line C is a central line from interdimer coupling (see text).



**Figure 2.** Temperature dependence of zero-field splitting under atmospheric and high hydrostatic pressure.

spin-forbidden half-field transition ( $\Delta M_s = \pm 2$ ), and (c) the appearance of a central line (marked as C) at about 310 mT, which grows in intensity. When hydrostatic pressure is applied, merely effect c appears. Thus, the  $\mathbf{D}$  tensor is pressure independent within experimental error. It is presented in Figure 2, where  $D(T)$  data for two pressures are shown.

The  $\text{CuCl}_4^{2-}$  complexes in our crystal have a pseudotetrahedral geometry with the flattening angle  $2\gamma = \text{Cl}-\text{Cu}-\text{Cl} = 147^\circ$  in approximately  $D_{2d}$  symmetry.<sup>2</sup> Thus, the geometry deviates from a free  $\text{CuCl}_4^{2-}$  geometry ( $2\gamma = 123^\circ$ ) as a result of lattice forces or a strain resulting from dimer formation.

Square-planar  $\text{CuCl}_4^{2-}$  complexes are known to undergo second-order Jahn-Teller interactions in such a way that the potential surface has the lowest symmetrical minimum in the ground state and two additional minima in the excited state corresponding to two distorted-tetrahedral geometries of  $b_{2u}$  vibrations. The relative heights of these minima are reflected in the temperature dependence of electronic spectra and spin Hamiltonian parameters.<sup>5,6</sup> In dinuclear species such as  $\text{Cu}_2\text{Cl}_6^{2-}$  this pattern can be more complicated, for instance making the two excited minima non-equivalent and lowering the symmetry of the ground state, despite

the fact that the electronic structure observed by optical absorption spectra for mononuclear  $\text{CuCl}_4^{2-}$  complexes is not strongly affected by a  $\text{Cu}_2\text{Cl}_6$  dimer formation.<sup>7</sup> The Jahn-Teller activity, however, should result in the temperature dependence of the electronic parameters. This is indeed what we observed in  $[(\text{C}_6\text{H}_5)_4\text{Sb}]_2\text{Cu}_2\text{Cl}_6$  by EPR spectroscopy.

The EPR parameter that most clearly shows a temperature dependence is  $D$ . The  $g$  factors also seem to be temperature dependent. They are, however, determined from powder spectra with less accuracy. The  $D$  parameter has already been found to be mainly determined by anisotropic exchange;<sup>2</sup> therefore, it seems reasonable to attribute the temperature variation of  $D$  to the change in population of the vibronic levels, which must be characterized by different anisotropic exchange integrals. Indeed, for a square-planar geometry the magnetic orbital is  $xy$  and  $D_{zz} = 1/3(g_z - g_0)^2 J_{xy,x^2-y^2}^{\text{an}}$ , where  $J^{\text{an}}$  represent coupling between the ground state of the first ion and the excited  $x^2 - y^2$  state of the second ion.<sup>8,9</sup>  $J_{xy,x^2-y^2}^{\text{an}}$  is expected to be strongly ferromagnetic. When the planar geometry is deformed toward a tetrahedron, we have an admixture of  $x^2 - y^2$  and  $xz$  in the ground state. This mixing exists in vibronic levels and produces a decrease of the effective  $J^{\text{an}}$  value since much smaller values are expected for both  $J_{x^2-y^2,x^2-y^2}$  and  $J_{xz,x^2-y^2}$  couplings. Thus, the maximum anisotropic exchange appears in the planar geometry and decreases with tetrahedral deformation, yielding variations in  $D$ . This is what we observe as a linear decrease of  $D$  on heating.

A confirmation of this model comes from the observed pressure independence of  $D$ , since a hydrostatic pressure lower than gigapascals does not affect molecular vibrations.<sup>10</sup> Thus, our crystal represents a rare case where a physical parameter is affected by temperature but not by pressure.

The interdimer exchange coupling  $J_1$  is very weak in our crystal, as is proved by resolved fine-structure lines. This coupling, however, influences, our EPR spectra. An effect of the interdimer coupling becomes evident as an appearance of the central line in the powder spectrum (Figure 1). This line is due to the merging effect between EPR lines split less than about  $0.3J_1$ . The  $J_1$  value can be estimated by the method of ref 11 and 12 as equal to  $J_1 = 0.005 \text{ cm}^{-1}$  at room temperature. The central line intensity increases on cooling and under pressure, indicating that the interdimer coupling increases with a shortening of intermolecular distances similarly to that observed in other chloro-bridged  $\text{Cu(II)}$  dimers.<sup>13</sup>

**Acknowledgment.** This work was partially supported by the Polish Academy of Sciences (Project CPBP 01.12). The financial support of the Italian Ministry of Public Education is gratefully acknowledged.

**Registry No.**  $[(\text{C}_6\text{H}_5)_4\text{Sb}]_2\text{CuCl}_6$ , 67597-60-8.

- (7) Desjardins, S. R.; Wilcox, D. E.; Musselman, R. L.; Solomon, E. I. *Inorg. Chem.* **1987**, *26*, 288.
- (8) Banci, L.; Bencini, A.; Gatteschi, D. *J. Am. Chem. Soc.* **1983**, *105*, 701.
- (9) Chow, C.; Willett, R. D. *J. Chem. Phys.* **1973**, *59*, 5903.
- (10) Drickamer, H. R. *Acc. Chem. Res.* **1986**, *19*, 329.
- (11) Hoffmann, S. K. *Chem. Phys. Lett.* **1983**, *98*, 329.
- (12) Hilczner, W.; Hoffmann, S. K. *Chem. Phys. Lett.* **1988**, *144*, 199.
- (13) Hoffmann, S. K.; Towle, D. K.; Hatfield, W. E.; Chaudhuri, P.; Wieghardt, K. *Inorg. Chem.* **1985**, *24*, 1307.

Contribution from the Institut für Anorganische und Analytische Chemie, Freie Universität Berlin, Fabeckstrasse 34-36, D-1000 Berlin 33, West Germany

#### Formation of Reactive Cationic Iron Clusters by Halogen Exchange and Abstraction from Nonacarbonylbis( $\mu_3$ -fluoromethylidyne)triiron with Lewis Acids

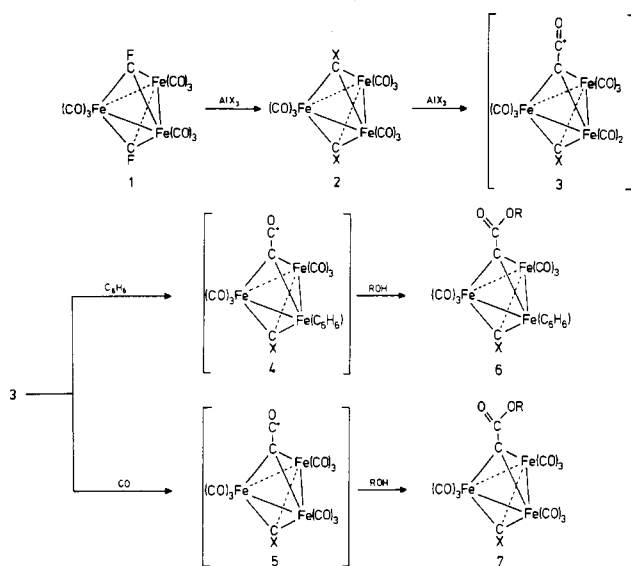
Dieter Lentz\* and Heike Michael

Received December 15, 1988

Nonacarbonylbis( $\mu_3$ -alkylidyne)triiron clusters have been of great recent interest.<sup>1-7</sup> In order to study the limits of stability

- (1) Hatfield, W. E. In *Magneto-Structural Correlations in Exchange Coupled System*; Willett, R. D., Gatteschi, D., Kahn, O., Eds.; Reidel: Dordrecht, Holland, 1985.
- (2) Bencini, A.; Gatteschi, D.; Zanchini, C. *Inorg. Chem.* **1985**, *24*, 704.
- (3) Stankowski, J.; Maćkowiak, M.; Krupski, M. *Sci. Instrumentation* **1986**, *1*, 3.
- (4) Stankowski, J.; Gałęzowski, A.; Krupski, M.; Wapłak, S.; Gierszal, H. *Rev. Sci. Instrum.* **1976**, *47*, 128.
- (5) McDonald, R. G.; Riley, M. J.; Hitchman, M. A. *Inorg. Chem.* **1988**, *27*, 3205.
- (6) Riley, M. J.; Hitchman, M. A. *Inorg. Chem.* **1987**, *26*, 3205.

Scheme I



of bis( $\mu_3$ -alkylidene)triiron clusters vs the isomeric alkyne clusters, we were interested in using the nonacarbonylbis( $\mu_3$ -fluoromethylidene)triiron cluster<sup>2</sup> (**1**) as a starting material for the preparation of bis( $\mu_3$ -alkylidene)triiron clusters.

Dolby and Robinson reported that  $\text{Co}_3(\text{CO})_9(\mu_3\text{-CCl})$  can be used as a Friedel Crafts alkylation reaction forming  $\text{Co}_3(\text{CO})_9(\mu_3\text{-C-R})$  ( $\text{R} = \text{aryls}$ ).<sup>8</sup>

In our attempt to extend this reaction to  $\text{Fe}_3(\text{CO})_9(\mu_3\text{-CF})_2$  (**1**) using  $\text{AlCl}_3$  in benzene, we have observed the formation of  $\text{Fe}_3(\text{CO})_9(\mu_3\text{-CCl})_2$  (**2**) at ambient temperature. The structure of  $\text{Fe}_3(\text{CO})_9(\mu_3\text{-CCl})_2$  (**2**) has been confirmed by its spectroscopic data, which are very similar to those of  $\text{Fe}_3(\text{CO})_9(\mu_3\text{-CF})_2$ .

On heating of the reaction mixture to reflux or by the use of  $\text{AlBr}_3$ , a further attack of  $\text{Fe}_3(\text{CO})_9(\mu_3\text{-CX})_2$  ( $\text{X} = \text{Cl}, \text{Br}$ ) occurs, resulting in a brown precipitate, which is insoluble in nonpolar solvents. With alcohols, however, a further reaction takes place yielding  $\text{Fe}_3(\text{CO})_6(\eta^6\text{-C}_6\text{H}_6)(\mu_3\text{-CX})(\mu_3\text{-C-COOR})$  ( $\text{X} = \text{Cl}, \text{R} = \text{C}_2\text{H}_5$  (**6a**);  $\text{X} = \text{Br}, \text{R} = \text{CH}_3$  (**6b**)), whose formation can easily be explained by the mechanism shown in Scheme I.

Attack of **2** by a Lewis acid results in a polarization of the carbon-halogen bond of **2** or in the formation of the cationic species. Migration of a carbonyl ligand to the electrophilic carbon atom creates a vacant site in the coordination sphere of one iron atom, forming the cationic ketenylidene cluster **3**. This vacant site can be occupied by benzene, resulting in an elimination of 2 mol of carbon monoxide, forming the cationic ketenylidene cluster **4**, which contains an  $\eta^6$ -coordinated benzene ligand. Obviously, the electrophilicity of **4** is too low for an electrophilic attack of the benzene ring. On reaction with the more nucleophilic alcohol, however, formation of the ester **6a,b** occurs.

If this proposed mechanism is correct, **3** should react with other ligands as for example carbon monoxide, yielding **5**.

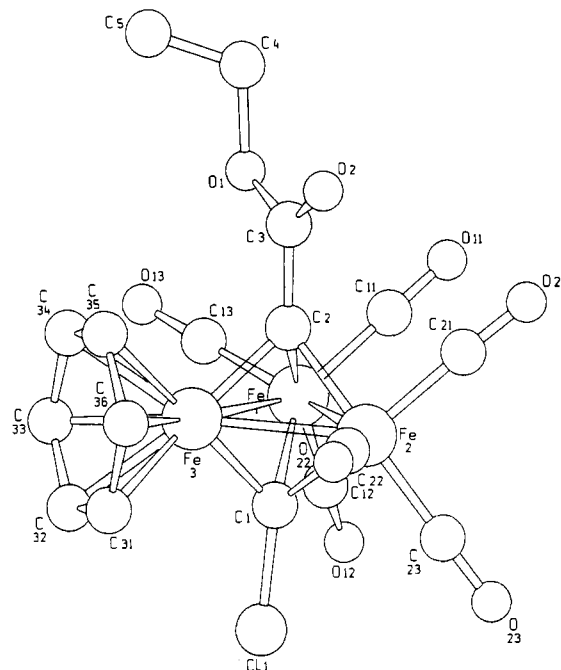


**Figure 1.** SCHAKAL plot of **6a**. Important bond lengths (pm) and angles (deg) are as follows: Fe1-Fe2 = 252.2 (2), Fe1-Fe3 = 250.0 (2), Fe2-Fe3 = 250.0 (2), Fe1-C1 = 195.4 (5), Fe1-C2 = 195.6 (2), Fe2-C1 = 193.6 (5), Fe2-C2 = 194.6 (5), Fe3-C1 = 184.3 (5), Fe3-C2 = 187.9 (5), Fe-CO = 177.5 (6)-180.5 (6), C-O = 113.0 (7)-114.8 (7), Fe3-C(benzene) = 210.7 (10)-212.8 (7), C1-C11 = 175.7 (5), C2-C3 = 148.0 (7), C3-O1 = 133.2 (7), C3-O2 = 118.1 (7), C4-O1 = 147.7 (9), C4-C5 = 140.0 (11), Fe2-Fe1-Fe3 = 59.69 (3), Fe1-Fe2-Fe3 = 59.72 (3), Fe1-Fe3-Fe2 = 60.58 (3), C1-Fe1-C2 = 80.1 (2), C1-Fe2-C2 = 80.8 (2), C1-Fe3-C2 = 85.1 (2), Fe1-C1-Fe2 = 80.8 (2), Fe1-C1-Fe3 = 82.3 (2), Fe2-C1-Fe3 = 82.8 (2), Fe1-C1-C11 = 131.5 (3), Fe2-C1-C11 = 131.2 (3), Fe3-C1-C11 = 129.6 (3), Fe1-C2-Fe2 = 80.5 (2), Fe1-C2-Fe3 = 81.4 (2), Fe2-C2-Fe3 = 81.6 (2), Fe1-C2-C3 = 132.6 (4), Fe2-C2-C3 = 132.3 (4), Fe3-C2-C3 = 129.0 (4), C2-C3-O1 = 112.5 (5), C2-C3-O2 = 125.4 (5), O1-C3-O2 = 122.1 (5).

Carrying out this reaction in dichloromethane in the presence of carbon monoxide yields the intermediate compound **5**, whose infrared spectrum shows four absorptions at 2160 (w), 2139 (s), 2094 (vs), and 2053 (s)  $\text{cm}^{-1}$ . Apart from a shift of the absorptions to higher wavenumbers, which is due to the positive charge, this infrared spectrum closely resembles that of  $[\text{Os}_3(\text{CO})_9(\mu_3\text{-CCO})]^{2-}$ .<sup>9</sup> Reaction with methanol yields  $\text{Fe}_3(\text{CO})_9(\mu_3\text{-CBr})(\mu_3\text{-C-COOCH}_3)$  (**7**). Further support for the above mechanism comes from the fact that the cation  $\text{Co}_3(\text{CO})_9(\mu_3\text{-CCO})^+$  has been isolated by Seyferth et al.<sup>10</sup> This cation yields similar products on the reaction with nucleophiles.<sup>10,11</sup> In addition, similar reactions of  $\mu_3$ -bromomethylidene clusters of ruthenium<sup>12</sup> and osmium<sup>13</sup> with aluminum trichloride have been reported.

The structure of  $\text{Fe}_3(\text{CO})_6(\eta^6\text{-C}_6\text{H}_6)(\mu_3\text{-CCl})(\mu_3\text{-C-COOC}_2\text{H}_5)$  (**6a**) has been the subject of an X-ray crystal structure analysis (Figure 1, Table I). The iron atoms of **6a** form a nearly regular triangle. The Fe-Fe distance between the two  $\text{Fe}(\text{CO})_3$  units is only slightly longer than the other Fe-Fe distances. The Fe-C distances of the  $\text{Fe}(\text{CO})_3$  units bound to the alkyldiene carbon atoms are very similar (193.6-195.6 (5) pm). The Fe-C distances involving the  $\text{Fe}(\text{C}_6\text{H}_6)$  unit of Fe3-C1 = 184.3 (5) and Fe3-C2 = 187.9 (5) pm are significantly shorter. However, this asymmetry of the  $\mu_3$ -bridges is much less distinct than in  $\text{Fe}_3(\text{CO})_9(\mu_3\text{-$

- Wong, W.-K.; Chiu, K. W.; Wilkinson, G.; Galas, A. M.-R.; Thornton-Pett, M.; Hursthouse, M. B. *J. Chem. Soc., Dalton Trans.* **1983**, 1557.
- Lentz, D.; Brüdgam, I.; Hartl, H. *Angew. Chem.* **1985**, *97*, 115; *Angew. Chem., Int. Ed. Engl.* **1985**, *24*, 119. Lentz, D.; Michael, H. *Chem. Ber.* **1988**, *121*, 1413. Lentz, D.; Michael, H. *Angew. Chem.* **1988**, *100*, 871; *Angew. Chem., Int. Ed. Engl.* **1988**, *27*, 845. Lentz, D.; Michael, H. *Angew. Chem.* **1989**, *101*, 330; *Angew. Chem., Int. Ed. Engl.* **1989**, *28*, 321.
- Nuel, D.; Dahan, F.; Mathieu, R. *J. Am. Chem. Soc.* **1985**, *107*, 1658.
- Hriljac, J. A.; Shriver, D. F. *J. Am. Chem. Soc.* **1987**, *109*, 6010.
- Cabrera, E.; Daran, J. C.; Jeannin, Y. *J. Chem. Soc., Chem. Commun.* **1988**, 607.
- Nuel, D.; Mathieu, R. *Organometallics* **1988**, *7*, 16. Suades, J.; Dahan, F.; Mathieu, R. *Organometallics* **1988**, *7*, 47.
- Aradi, A. A.; Grevels, F.-W.; Krüger, C.; Raabe, E. *Organometallics* **1988**, *7*, 812.
- Dolby, R.; Robinson, B. H. *J. Chem. Soc., Chem. Commun.* **1970**, 1058; *J. Chem. Soc., Dalton Trans.* **1972**, 2046.

- Went, M. J.; Sailor, M. J.; Bogdan, P. L.; Brock, C. P.; Shriver, D. F. *J. Am. Chem. Soc.* **1987**, *109*, 6023.
- Seyferth, D.; Hallgren, J. E.; Eschbach, C. S. *J. Am. Chem. Soc.* **1974**, *96*, 1730.
- Seyferth, D.; Williams, G. H.; Nivert, C. L. *Inorg. Chem.* **1977**, *16*, 758.
- Keister, J. B.; Horling, T. L. *Inorg. Chem.* **1980**, *19*, 2304.
- Sievert, A. C.; Strickland, D. S.; Shapley, J. R.; Steinmetz, G. R.; Geoffroy, G. L. *Organometallics* **1982**, *1*, 214.

**Table I.** Crystallographic Data for  $\text{Fe}_3(\text{CO})_6(\eta^6\text{-C}_6\text{H}_6)(\mu_3\text{-C-Cl})(\mu_3\text{-C-COOC}_2\text{H}_5)$ 

chem formula $\text{C}_{17}\text{H}_{11}\text{ClFe}_3\text{O}_8$	fw 546.26
$a = 8.973$ (4) Å	space group $P2_1/c$ (No. 14)
$b = 9.441$ (3) Å	$T = 20$ °C
$c = 23.615$ (5) Å	$\lambda = 0.71069$ Å
$\beta = 96.53$ (3) deg	$\mu(\text{Mo K}\alpha) = 23.84$ cm <sup>-1</sup>
$V = 1987.5$ Å <sup>3</sup>	$R(F_o) = 0.038$
$Z = 4$	$R_w(F_o) = 0.038$ ( $w = 1$ )
$d_{\text{calc}} = 1.82$ g cm <sup>-3</sup>	

$\text{CMe}(\mu_3\text{-C-NEt}_2)$ , which possesses a very asymmetric C-NEt<sub>2</sub> bridge.<sup>5</sup>

In the <sup>13</sup>C NMR spectrum of all of these compounds, the carbonyl carbon atoms give rise to only one singlet, thus indicating that they are equivalent on the NMR time scale. This is consistent with a nonrigid structure of the  $\text{Fe}(\text{CO})_3$  units in solution.

None of these bis(alkylidyne)triiron clusters has shown any evidence of isomerization to the corresponding alkyne cluster. Further studies concerning the reactivity of  $\text{Fe}_3(\text{CO})_9(\mu_3\text{-CF})_2$  are in progress.

### Experimental Section

**Material.** Nonacarbonylbis(fluoromethylidyne)triiron was prepared by literature procedures.<sup>2</sup> Aluminum chloride (Merck) and aluminum bromide (Merck) were used as received. All experiments were carried out under argon by using standard Schlenk and vacuum-line techniques.

**Synthesis of  $\text{Fe}_3(\text{CO})_9(\mu_3\text{-CF})_2$  (2).** A 460-mg amount (0.96 mmol) of  $\text{Fe}_3(\text{CO})_9(\mu_3\text{-CF})_2$  (1) was dissolved in 50 mL of benzene. An excess of  $\text{AlCl}_3$  was added, and the reaction mixture was stirred for 20 min at ambient temperature. The end of the reaction was monitored by <sup>19</sup>F NMR spectroscopy. After filtration, the solvent was removed under vacuum. The residue was dissolved in  $\text{CH}_2\text{Cl}_2$ , and the mixture was filtered through a layer of silica (5 cm). Elution with  $\text{CH}_2\text{Cl}_2$  and recrystallization from *n*-pentane yielded 233 mg (47%) of red crystalline 2.

**Synthesis of  $\text{Fe}_3(\text{CO})_6(\eta^6\text{-C}_6\text{H}_6)(\mu_3\text{-CCl})(\mu_3\text{-CCOOC}_2\text{H}_5)$  (6a).** An excess of  $\text{AlCl}_3$  (0.5 g) was added to a solution of 100 mg (0.2 mmol) of 1 in 50 mL of benzene. The reaction mixture was refluxed for 1 h. After cooling to ambient temperature, an excess of ethanol (15 mL) was added. The solution was stirred for 40 min at ambient temperature. After removal of the solvent in vacuum the residue was dissolved in  $\text{CH}_2\text{Cl}_2$  and the mixture filtered through a 5-cm layer of silica. The solvent was removed in vacuum, and the residue was recrystallized from *n*-pentane solution at -20 °C, yielding 25 mg (25%) of brown crystalline 6a.

**Synthesis of  $\text{Fe}_3(\text{CO})_6(\eta^6\text{-C}_6\text{H}_6)(\mu_3\text{-CBr})(\mu_3\text{-CCOOC}_2\text{H}_5)$  (6b).** A 103-mg amount (0.21 mmol) of  $\text{Fe}_3(\text{CO})_9(\mu_3\text{-CF})_2$  was dissolved in 50 mL of benzene. After the addition of an excess of  $\text{AlBr}_3$  the orange solution immediately turned dark brown. After 40 min at ambient temperature 10 mL of methanol was added, resulting in a red solution. The reaction was stirred for 2 h at ambient temperature, and the solvents were removed under vacuum. The residue was dissolved in dichloromethane and the solution filtered through a layer of silica (3 cm) using dichloromethane as an eluent. The solvent was removed under vacuum. After addition of 10 mL of *n*-pentane, 6b was obtained as dark red crystals (27 mg, 22.5%).

**Synthesis of  $\text{Fe}_3(\text{CO})_9(\mu_3\text{-CBr})(\mu_3\text{-CCOOC}_2\text{H}_5)$  (7).** A 350-mg amount (0.73 mmol) of  $\text{Fe}_3(\text{CO})_9(\mu_3\text{-CF})_2$  (1) was dissolved in 60 mL of  $\text{CH}_2\text{Cl}_2$ . An excess of  $\text{AlBr}_3$  was added under a continuous CO purge. The solution was stirred for 20 min at ambient temperature. The end of the reaction was monitored by TLC on silica using  $\text{CH}_2\text{Cl}_2$  as eluent. An excess of methanol (2 mL) was added to this dark solution, which becomes deep red. After 1 h the solution was filtered through a layer of silica (5 cm). The solvent was removed in vacuo. The residue was dissolved in 20 mL of  $\text{CH}_2\text{Cl}_2$ , and approximately 4 g of silica was added. After the solvent was removed under vacuum, the residue was added to a 3-cm layer of silica in a short column. Elution with *n*-pentane gave a small amount of unreacted 1. 7 was eluted with  $\text{CH}_2\text{Cl}_2$  and recrystallized from *n*-pentane, yielding 253 mg (60%) of 7 as red crystals.

**Physical and Spectroscopic Data.**  $\text{Fe}_3(\text{CO})_9(\mu_3\text{-CCl})_2$  (2): red crystals, mp 145–150 °C dec. MS (80 eV):  $m/e$  514 ( $M^+$ ) followed by successive loss of nine CO ligands. IR ( $\text{CH}_2\text{Cl}_2$ ): 2060 (vs), 2040 (s), 2000 (m) cm<sup>-1</sup>. <sup>13</sup>C NMR ( $\text{CDCl}_3$ ): 206.3 (CO), 336.4 (CCl) ppm.  $\text{Fe}_3(\text{CO})_6(\eta\text{-C}_6\text{H}_6)(\mu_3\text{-CCl})(\mu_3\text{-C-COOC}_2\text{H}_5)$  (6a): brown crystals, mp 113–114 °C. MS (80 eV):  $m/e$  546 ( $M^+$ ) followed by successive loss of six CO ligands. IR (*n*-pentane): 2068 (vs), 2032 (vs), 2017 (s), 1982 (m), 1898 (w) cm<sup>-1</sup>. <sup>1</sup>H NMR ( $\text{CDCl}_3$ ): 5.69 ( $\text{C}_6\text{H}_6$ ), 4.86 ( $\text{CH}_2$ , <sup>3</sup>*J*<sub>HH</sub> = 7.1 Hz), 1.70 ( $\text{CH}_3$ ). <sup>13</sup>C[<sup>1</sup>H] NMR ( $\text{CDCl}_3$ ): 14.9 ( $\text{CH}_3$ ), 61.9 ( $\text{CH}_2$ ), 95.3 ( $\text{C}_6\text{H}_6$ ), 183.7 (COOEt), 210.5 (CO), 304.9 (C-COOEt), 339.4 ppm (CCl).  $\text{Fe}_3(\text{CO})_6(\eta\text{-C}_6\text{H}_6)(\mu_3\text{-CBr})(\mu_3\text{-C-COOC}_2\text{H}_5)$  (6b): red brown crystals, mp 125–128 °C dec. MS (80 eV):  $m/e$  576 ( $M^+$ ) followed by successive loss of six CO ligands. High-resolution MS of the molecular ion: calc,  $m/e$  575.7529; found,  $m/e$  575.7529. IR (*n*-pentane): 2093 (vw), 2062 (vs), 2034 (s), 2018 (m), 2005 (m), 1983 (w) cm<sup>-1</sup>. <sup>1</sup>H NMR ( $\text{CDCl}_3$ ): 5.69 ( $\text{C}_6\text{H}_6$ ), 4.39 ( $\text{CH}_3$ ) ppm. <sup>13</sup>C[<sup>1</sup>H] NMR ( $\text{CDCl}_3$ ): 53.1 ( $\text{CH}_3$ ), 95.5 ( $\text{C}_6\text{H}_6$ ), 184.5 (COOCH<sub>3</sub>), 210.3 (CO), 307.2 (C-COOMe), 329.7 (CBr) ppm.  $\text{Fe}_3(\text{CO})_9(\mu_3\text{-CBr})(\mu_3\text{-C-COOC}_2\text{H}_5)$  (7): red crystals, mp 115–116 °C. MS (80 eV):  $m/e$  582 ( $M^+$ ) followed by successive loss of nine CO ligands. High-resolution MS of the molecular ion: calc,  $m/e$  581.6907; found,  $m/e$  581.6904. IR (*n*-pentane): 2064 (vs), 2059 (vs), 2043 (s), 2038 (s), 2005 (m) cm<sup>-1</sup>. <sup>1</sup>H NMR ( $\text{CDCl}_3$ ): 4.30 ( $\text{CH}_3$ ) ppm. <sup>13</sup>C NMR ( $\text{CDCl}_3$ ): 53.7 ( $\text{CH}_3$ ), 181.0 (COOMe), 206.2 (CO), 316.6, 334.3 ppm.

**Crystal Structure Analysis.** Crystals were obtained by cooling an *n*-pentane solution of 6a. Crystal data: formula  $\text{C}_{17}\text{H}_{11}\text{ClFe}_3\text{O}_8$ , monoclinic,  $P2_1/c$ , No. 14,  $Z = 4$ ,  $a = 8.973$  (4) Å,  $b = 9.441$  (3) Å,  $c = 23.615$  (5) Å,  $\beta = 96.53$  (3)°,  $V = 1987.5$  Å<sup>3</sup>,  $d(\text{calc}) = 1.82$  g cm<sup>-3</sup>, Mo K $\alpha$  ( $\lambda = 0.71069$  Å). A total of 3495 independent reflections ( $\omega$  scan,  $2^\circ \leq \theta \leq 25^\circ$ ) were reduced to structure factors by correction for Lorentz and polarization effects. The structure was solved by direct methods, MULTAN. Anisotropic refinement of all non-hydrogen atoms by full-matrix least squares, XRAY 76, resulted in  $R = 0.038$  for 3098 reflections with  $F_o \geq 2\sigma(F_o)$ .

**Acknowledgment.** This research was supported by the Deutsche Forschungsgemeinschaft and the Fonds der Chemischen Industrie. We acknowledge Prof. Dr. J. Fuchs for his assistance in the crystallographic work.

**Supplementary Material Available:** For 6a, tables listing full crystallographic data, positional and thermal parameters, and interatomic distances and angles and a figure showing an ORTEP projection (6 pages); listings of observed and calculated structure factors (21 pages). Ordering information is given on any current masthead page.